Métodos de RMN no estado sólido

Jair C. C. Freitas

Programa de Pós-graduação em Física – UFES

Programa de Pós-graduação em Química - UFES

Sumário

- Técnicas de alta resolução em RMN de sólidos:
  - Ressonância dupla.
  - Desacoplamento heteronuclear.
  - Desacoplamento homonuclear.
  - Exemplos.

Interação dipolar internuclear

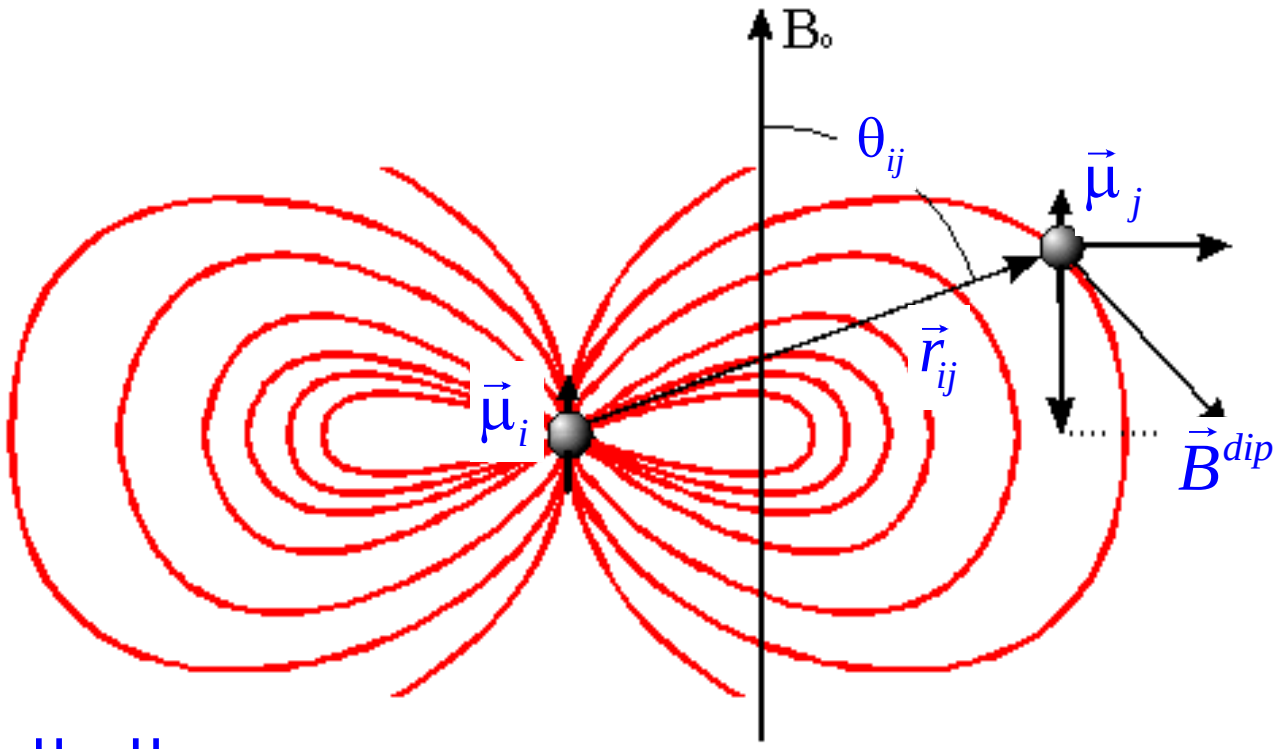

$$B_z^{dip} \cong \frac{\mu_0}{4\pi}\frac{\mu}{r_{ij}^3}(3\cos^2\theta_{ij} - 1)$$

Interação através do espaço

Interação dipolar internuclear

Par isolado de spins em um monocristal (caso heteronuclear):

$$\omega(\theta) = \omega_I \pm d\,\frac{3\cos^2\theta - 1}{2}$$

$$d = \frac{\mu_0}{4\pi}\,\frac{\gamma_I \gamma_S \hbar}{r^3}$$

$$d(3\cos^2\theta - 1)$$

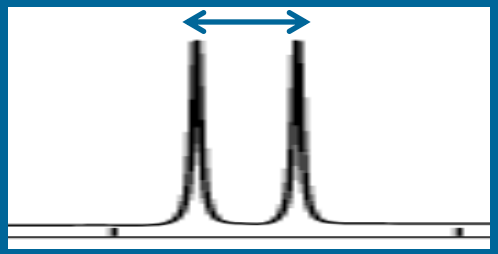

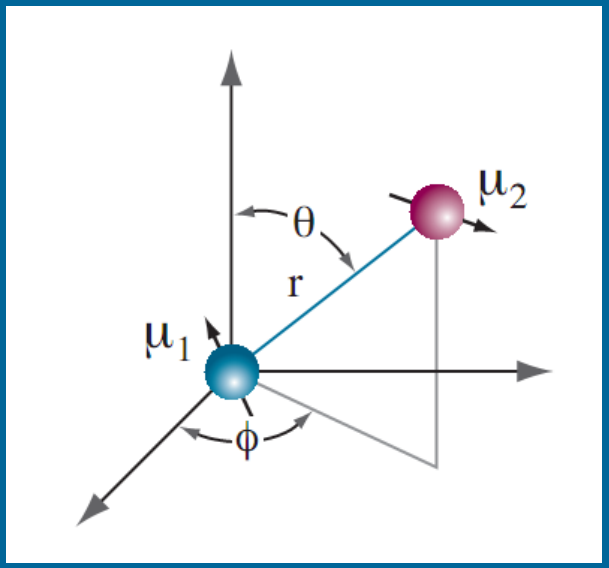

Desacoplamento dipolar heteronuclear

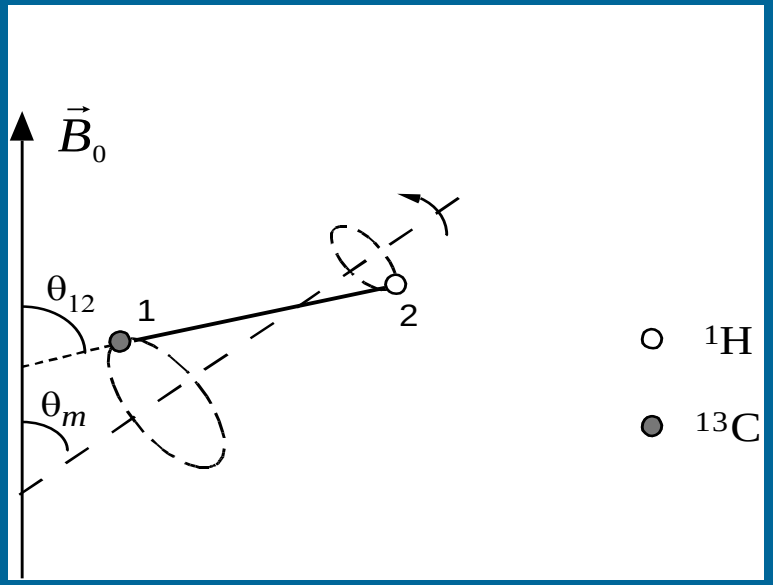

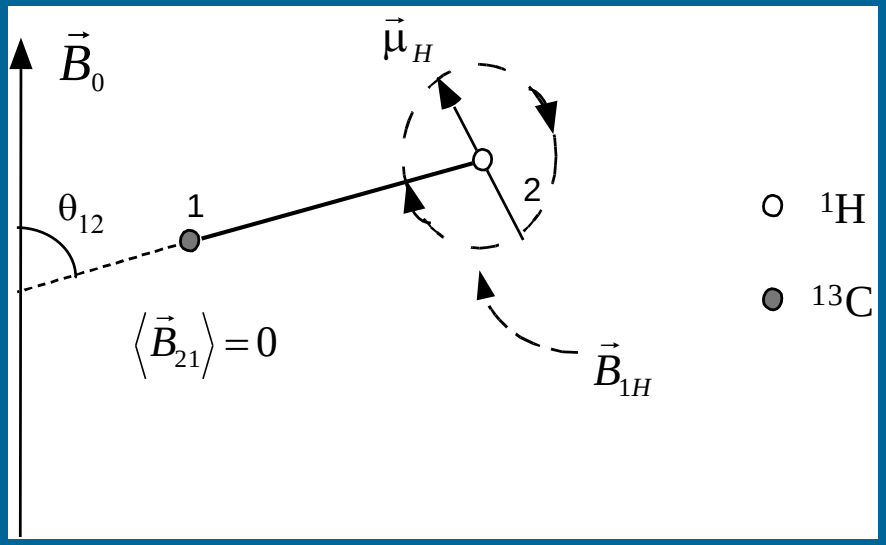

Ressonância dupla:

- Excitação de ^{1}H (f_{1H}) e de ^{13}C (f_{13C}).
- Detecção de ^{13}C (f_{13C}).

Desacoplamento dipolar heteronuclear

Eficiência do desacoplamento:

$$\gamma_H B_{1H} / 2\pi > \Delta f_{dip}$$

$$\Delta f_{dip} \sim d = \frac{\mu_0}{8\pi^2} \frac{\gamma_I \gamma_S \hbar}{r^3}$$

(alargamento devido ao acoplamento dipolar)

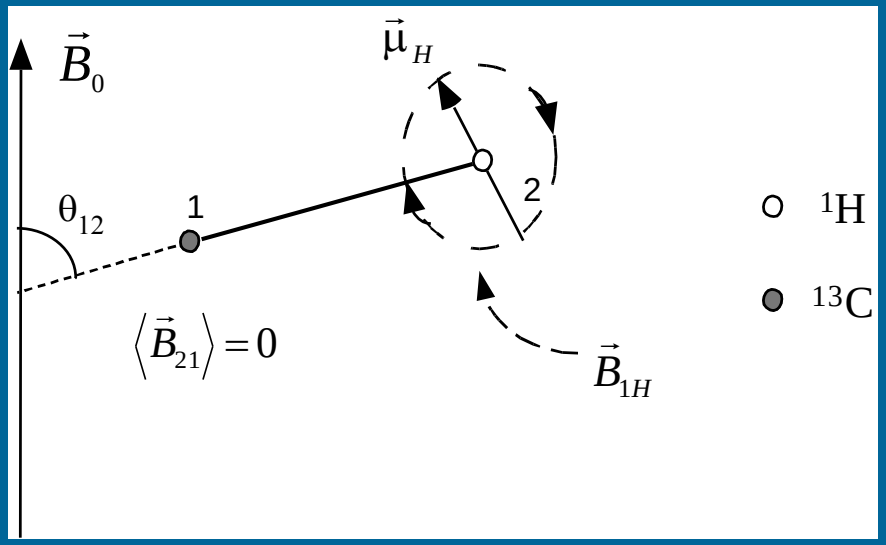

Par ^{1}H-^{13}C em grupo CH (ligação simples):

$$\Delta f_{dip} \sim 70 \text{ kHz}$$

Desacoplamento dipolar heteronuclear

Probe de ressonância dupla

Desacoplamento dipolar heteronuclear

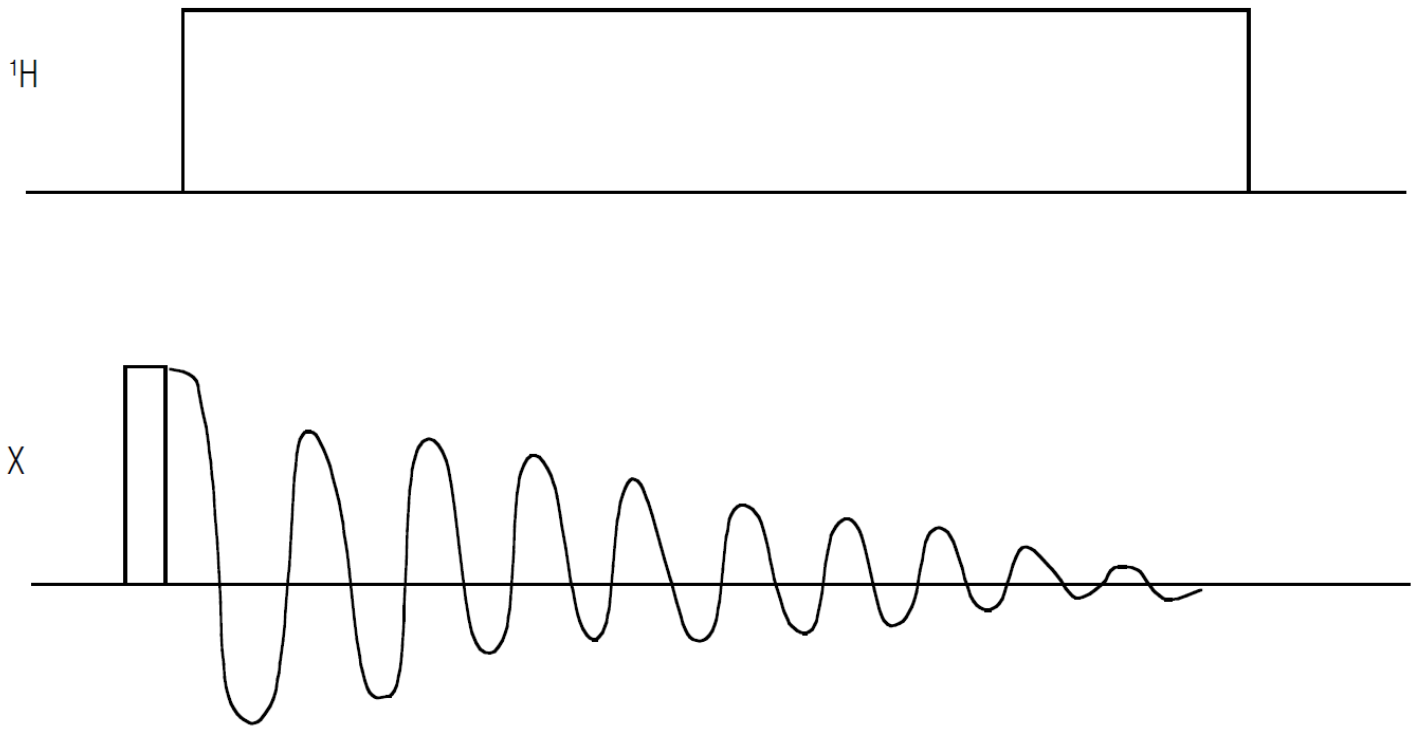

Fig. 2.7 High-power decoupling. This removes the effects of ^{1}H dipolar coupling from the NMR spectrum of X in this case; it can of course be applied to any abundant spin in place of ^{1}H in the same manner. High-power irradiation is simply applied to the ^{1}H spins during the acquisition of the X spin spectrum. Here a single pulse is used to generate the X transverse magnetization; this can of course be replaced with a more complicated preparation sequence. ^{1}H decoupling can also be used in the preparation sequence if necessary.

"Introduction to solid-state NMR spectroscopy", M. J. Duer. Blackwell, 2004.

Desacoplamento dipolar heteronuclear

RMN de ^{19}F (estado líquido) com desacoplamento de ^{1}H :

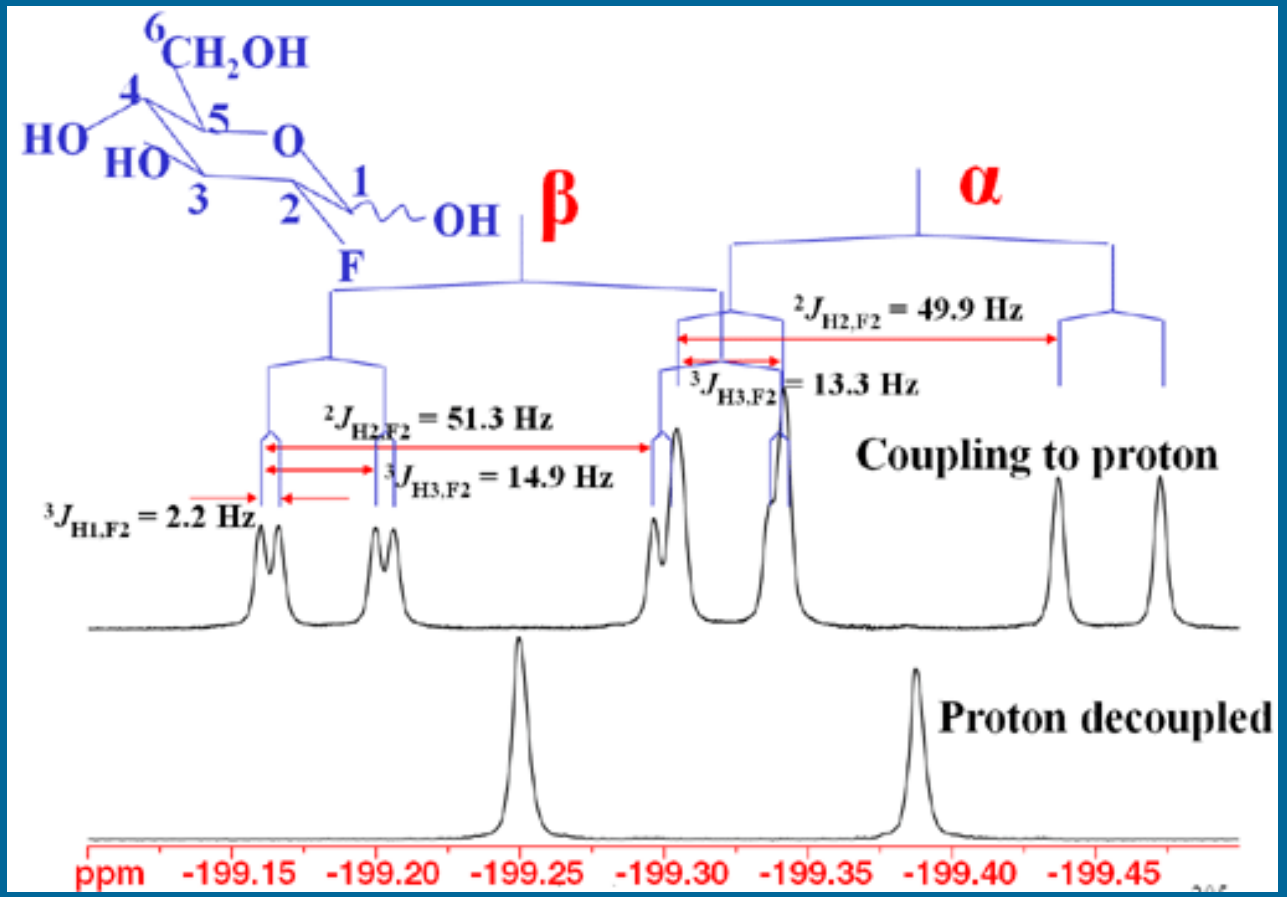

http://u-of-o-nmr-facility.blogspot.com/

Desacoplamento dipolar heteronuclear

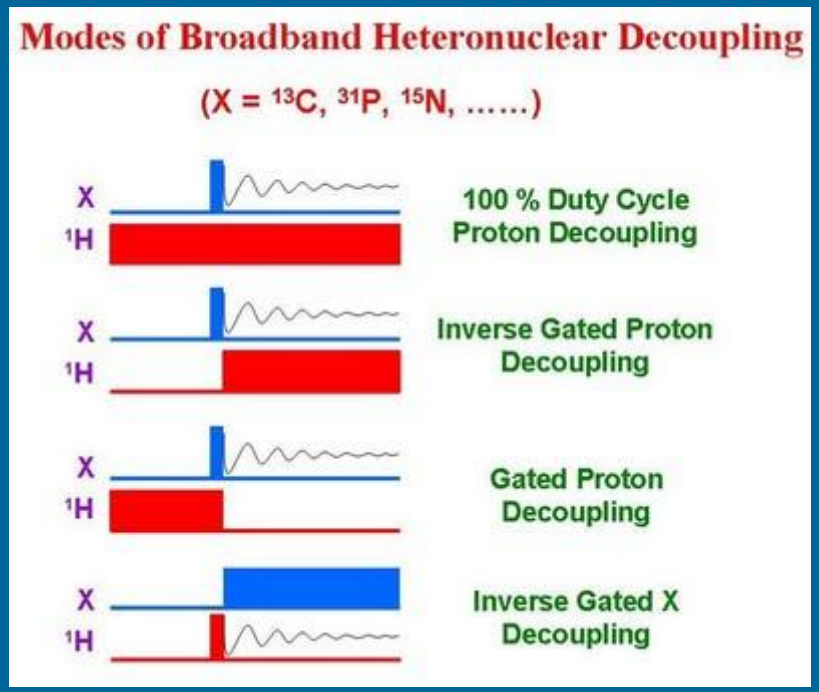

Espectros de RMN de ^{13}C com desacoplamento de ^{1}H:

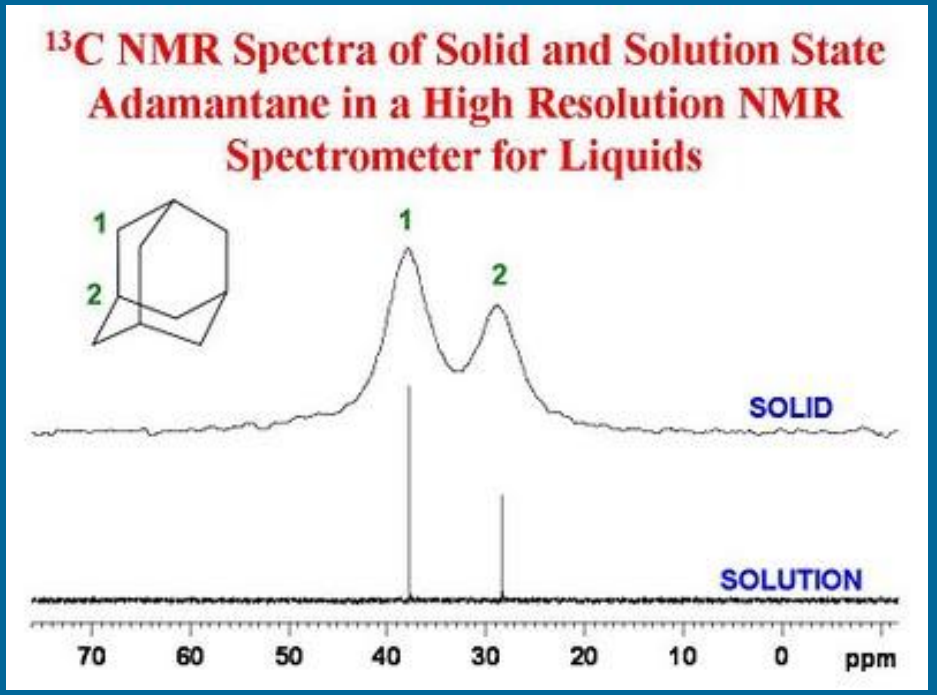

http://u-of-o-nmr-facility.blogspot.com/

Desacoplamento dipolar heteronuclear

Problemas com aquecimento da amostra:

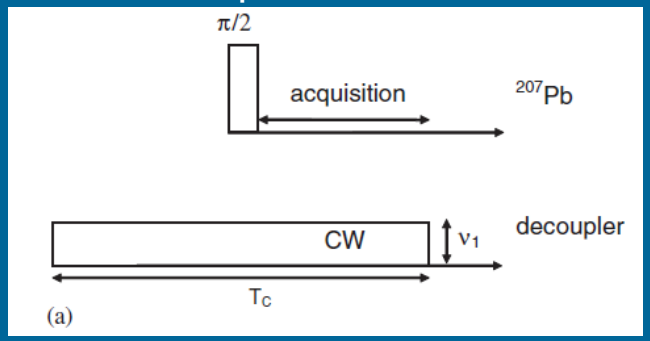

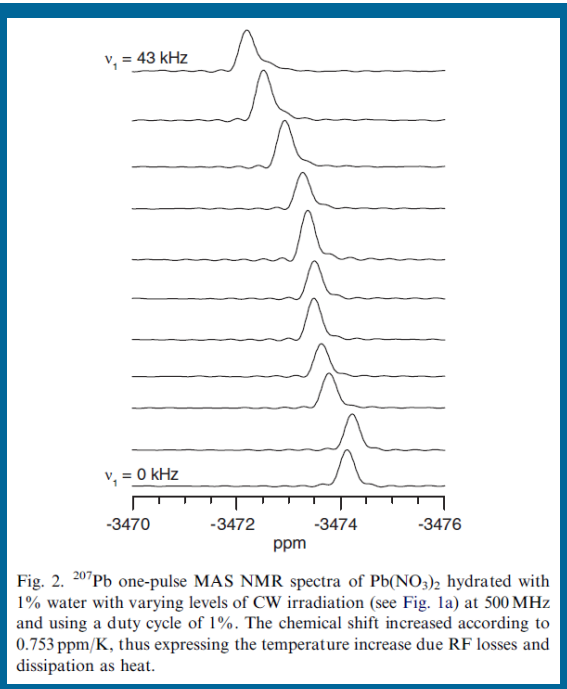

Fig. 2. ^{207}Pb one-pulse MAS NMR spectra of $Pb(NO_3)_2$ hydrated with 1% water with varying levels of CW irradiation (see Fig. 1a) at 500 MHz and using a duty cycle of 1%. The chemical shift increased according to 0.753 ppm/K, thus expressing the temperature increase due RF losses and dissipation as heat.

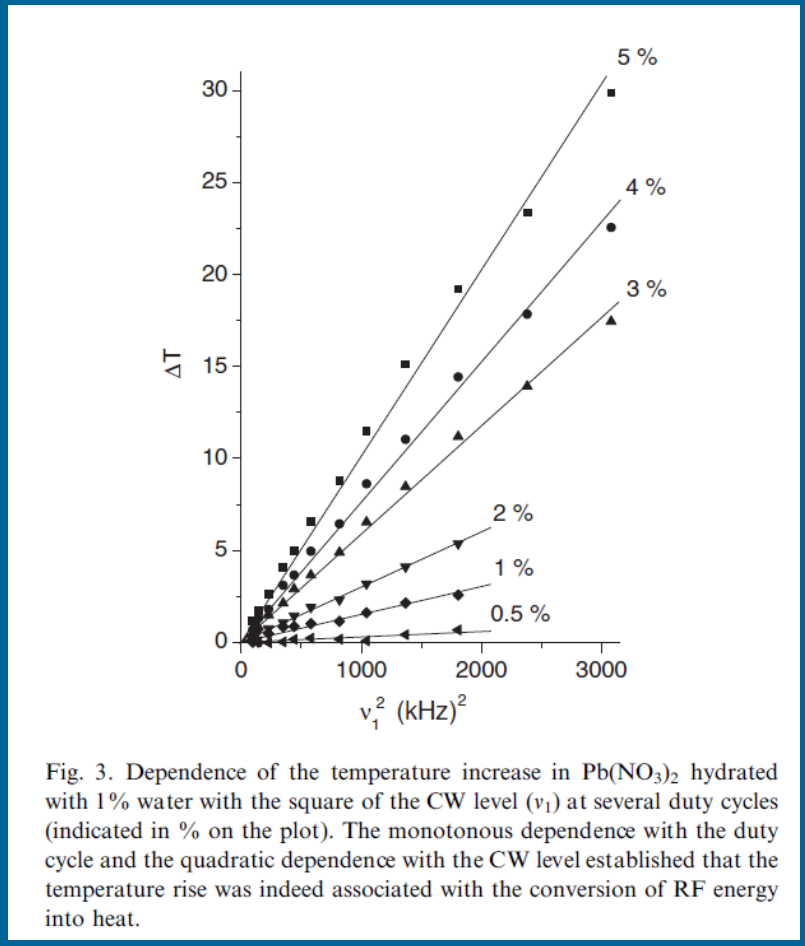

Fig. 3. Dependence of the temperature increase in $Pb(NO_3)_2$ hydrated with 1% water with the square of the CW level (ν_1) at several duty cycles (indicated in % on the plot). The monotonous dependence with the duty cycle and the quadratic dependence with the CW level established that the temperature rise was indeed associated with the conversion of RF energy into heat.

de Lacaillerie et al., Solid State Nucl. Magn. Reson. 2005;28:225.

Desacoplamento dipolar heteronuclear

Outras sequências de desacoplamento combinadas com MAS:

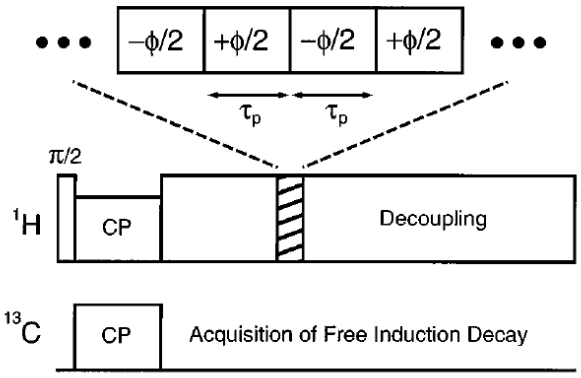

FIG. 1. Pulse sequence for the CPMAS experiment with the addition of phase modulated TPPM decoupling on the ^{1}H channel. A small hatched region of the decoupling period is expanded in order to illustrate the rapid alternation of the phase of the rf excitation between two values $-\phi/2$ and $+\phi/2$ with overall period $2\tau_p$, which is carried out throughout the acquisition of the FID.

TPPM = two pulse phase-modulation

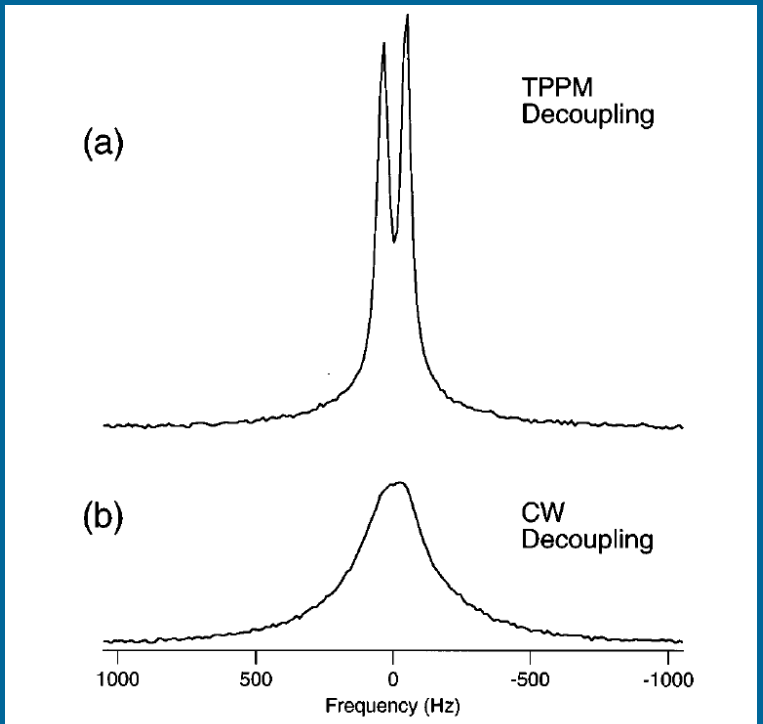

FIG. 3. The centerband of the CPMAS spectra of calcium formate at 10.7 kHz spinning frequency with (a) TPPM and (b) CW decoupling using the parameters: ϕ=75°, τ_p=7.5 μs. An rf field strength of 62.5 kHz (4.0 μs $\pi/2$ pulse length) was applied. The nonequivalent formate ions are separated by 80 Hz.

Bennett et al., J. Chem. Phys. 1995;103:6951.

MAS e acoplamento dipolar homonuclear

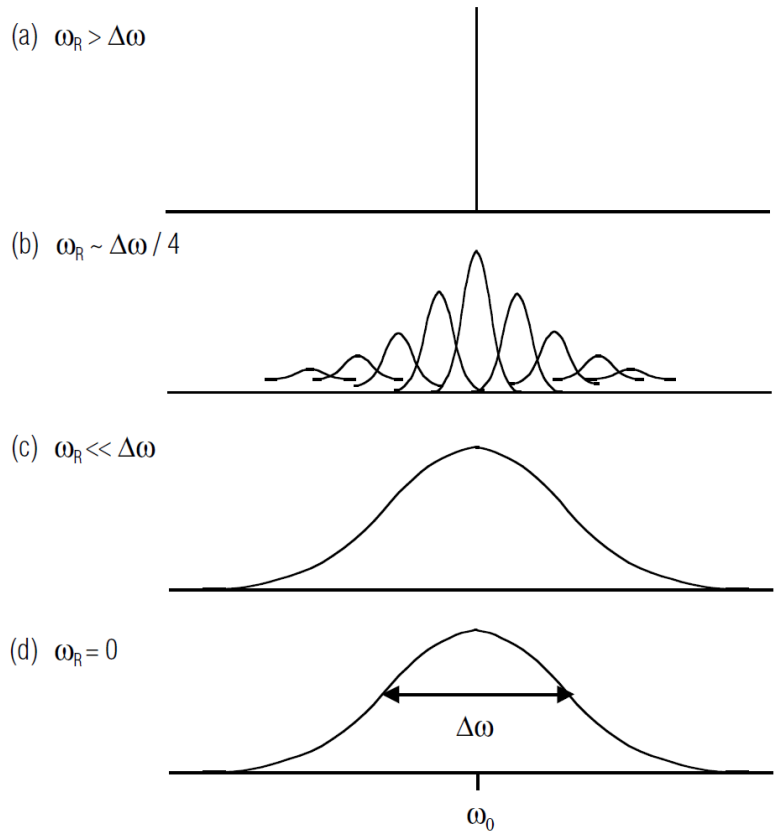

Fig. 2.6 The effects of magic-angle spinning on homonuclear dipole–dipole coupling. (a) The broad line which arises in the NMR spectrum (shown in (d)) from this interaction is only narrowed by magic-angle spinning for spinning rates of the order of the linewidth or greater. (b) For slower speeds, broad spinning sidebands appear, and (c) at still slower speeds, there is little effect on the spectrum at all.

"Introduction to solid-state NMR spectroscopy", M. J. Duer. Blackwell, 2004.

Desacoplamento dipolar homonuclear

Espectroscopia com sequência de múltiplos pulsos combinada com rotação (CRAMPS):

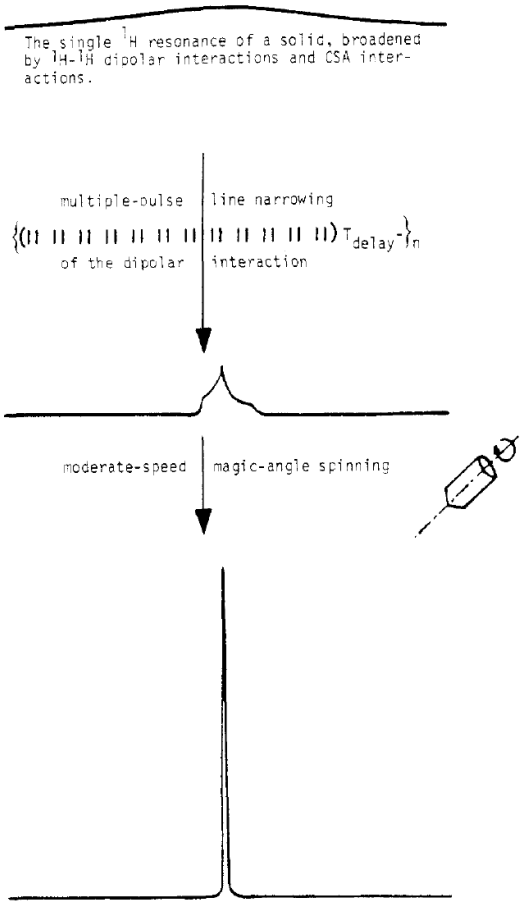

Figure 1. Diagram of the ^{1}H CRAMPS strategy.

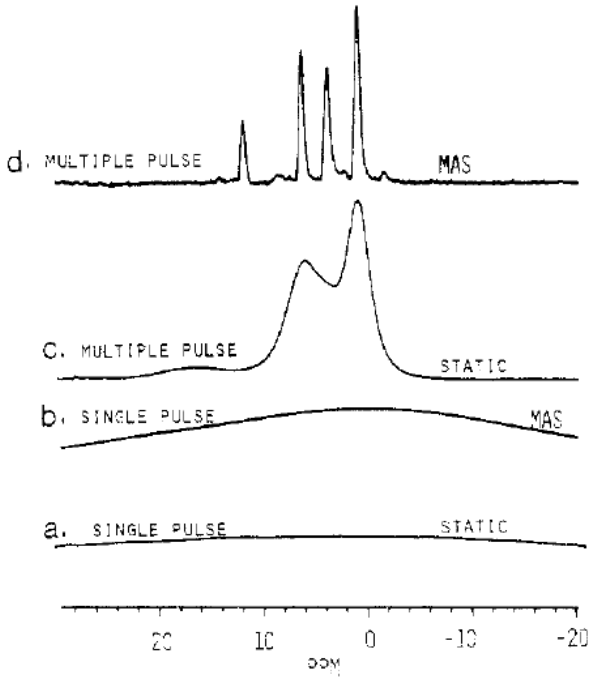

Figure 5. 187-MHz ^{1}H NMR spectra of $CH_3CH_2O_2CCH{=}CHCO_2H$: (a) result of a single-pulse experiment (many repetitions) on a static sample; (b) result of a single-pulse experiment on a sample undergoing magic-angle spinning; (c) result of a BR-24 multiple-pulse experiment on a static sample; (d) result of the ^{1}H CRAMPS experiment.

Bronnimann et al., Anal. Chem.1988;60:1743.

Desacoplamento dipolar homonuclear

Espectroscopia com sequência de múltiplos pulsos combinada com rotação (CRAMPS):

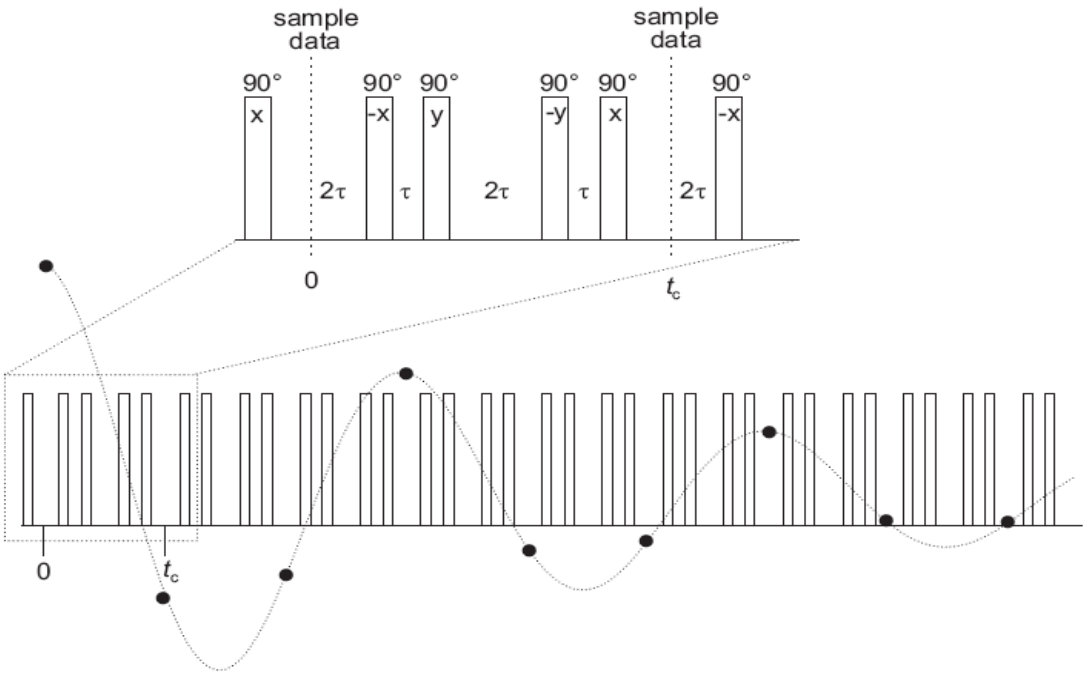

Figure 14: The WAHUHA pulse sequence for the CRAMPS experiment and the timing for data acquisition. The expanded region shows the details of the phase cycling and data sampling.

Bryce et al., Can. J. Anal. Sci. Spectr. 2001;46:46.

MAS e desacoplamento dipolar homonuclear

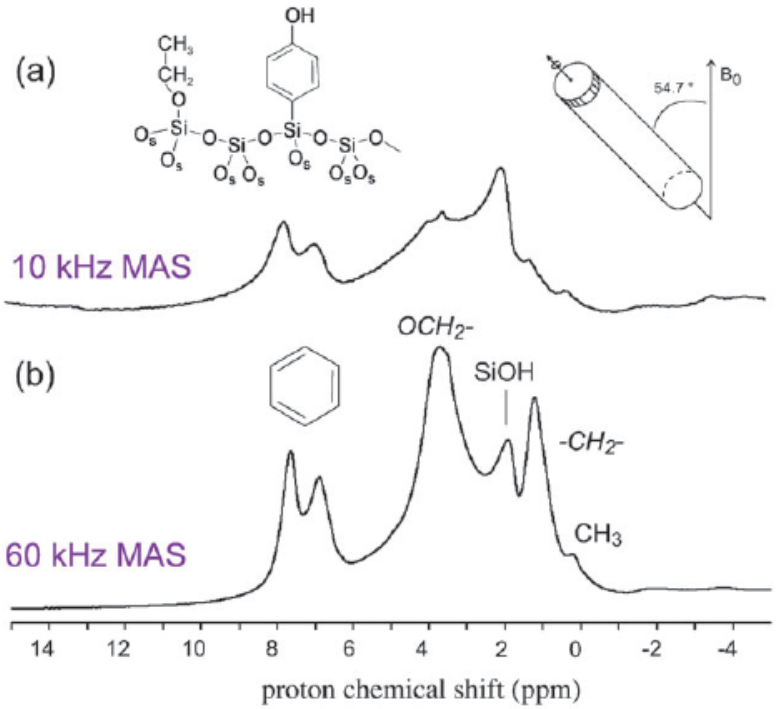

Fig. 1 One-dimensional ^{1}H spectra of an organic compound grafted inside the mesopores of a silica matrix, at 10 kHz (a) and 60 kHz MAS frequencies (resonances corresponding to surfactant chains are also observed). A total of 64 transients were recorded at a ^{1}H frequency of 900 MHz. The spectra were recorded using a 1.3 mm CPMAS probe (sample volume of 2 µL) on a Bruker Avance III spectrometer. (In collaboration with Dr C. Copéret and D. Gajan.)

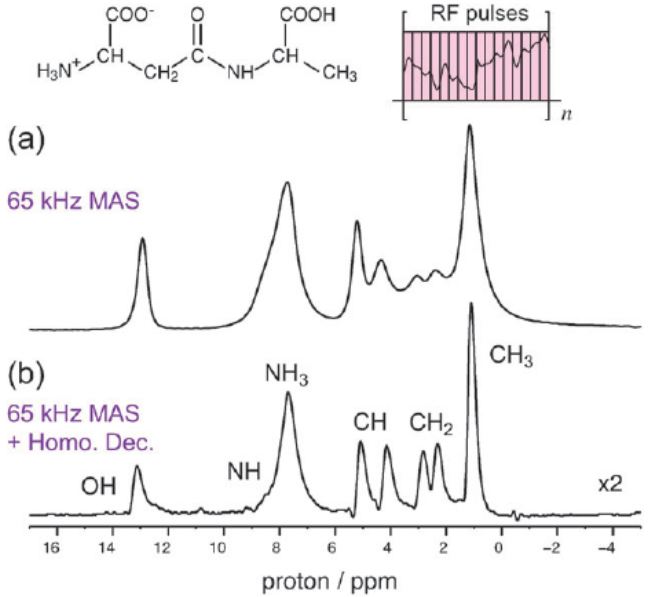

Fig. 2 One-dimensional ^{1}H spectra of the dipeptide b-L-Asp-L-Ala under MAS at 65 kHz. (a) MAS spectrum (2 transients). (b) Homonuclear-decoupled spectrum using the windowed eDUMBO-1_{22} sequence during direct acquisition (16 transients). eDUMBO-1_{22} was implemented with an RF pulse amplitude of 170 kHz. The homonuclear-decoupled spectrum shows a highly linear scaling factor (0.58) across the entire ^{1}H chemical shift range (as evaluated from the comparison between the decoupled and the MAS-only spectra). We note that windowed decoupling during acquisition compromises the overall spectral sensitivity. Reprinted from *Chem. Phys. Lett.*, 2009, **469**, E. Salager, R. S. Stein, S. Steuernagel, A. Lesage, B. Elena and L. Emsley. Enhanced sensitivity in high-resolution ^{1}H solid-state NMR spectroscopy with DUMBO dipolar decoupling under ultra-fast MAS, 336–341. Copyright 2009, with permission from Elsevier.[27]

Lesage, Phys. Chem. Chem. Phys. 2009;11:6876-6891

Bibliografia recomendada

- RMN de alta resolução em sólidos:
  - "Multinuclear solid-state NMR of inorganic materials", K. J. D. Mackenzie, M. E. Smith. Pergamon, 2002.
  - "High resolution NMR in solids", U. Haeberlen. In: *Adv. Magn. Reson. Suppl. I*, Academic Press, 1976.
  - "Introduction to solid-state NMR spectroscopy", M. J. Duer. Blackwell, 2004.
  - "NMR in rotating solids", M. M. Maricq, J. S. Waugh. *J. Chem. Phys.* 1979;70:3300-3316.
  - "Practical aspects of modern routine solid-state nuclear magnetic resonance spectroscopy: one-dimensional experiments", D. L. Bryce et al., *Can. J. Anal. Sci. Spectr.* 2001;46:46.
  - "Recent advances in experimental solid state NMR methodology for half-integer spin quadrupolar nuclei", M. E. Smith, E. R. H. van Eck. *Prog. Nucl. Magn. Reson. Spectr.* 1999;34:159-201.